Additive manufacturing of copper with a single mode IR fiber laser

Available online at www.sciencedirect.com

ScienceDirect

Procedia CIRP 118 (2023) 649–653

www.elsevier.com/locate/procedia

16th CIRP Conference on Intelligent Computation in Manufacturing Engineering, CIRP ICME '22, Italy

Additive manufacturing of copper with a single mode IR fiber laser

F. Calignano[a,*], M. Pavese[b], A. Saboori[a], M. Galati[a], L. Iuliano[a]

[a] Department of Management and Production Engineering (DIGEP), Integrated Additive Manufacturing Center (IAM), Politecnico di Torino, Corso Duca Degli Abruzzi, 24, 10129 Turin,, Italy

[b] Department of Applied Science and Technology (DISAT), Integrated Additive Manufacturing Center (IAM), Politecnico di Torino, Corso Duca Degli Abruzzi, 24, 10129 Turin,, Italy

* Corresponding author. Tel.: +39 0110907218; *E-mail address:* flaviana.calignano@polito.it

Abstract

Laser powder bed fusion (L-PBF) process was used to produce copper (Cu) and copper with graphene nanoplatelets (Cu-GNP) samples using a conventional single-mode IR fiber laser with a wavelength of 1060-1080 nm and power levels up to 500 W. Cu and Cu-GNP samples were fabricated considering the same process parameters in order to investigate the effect of GNP to increase the optical absorbency of Cu. It has been shown through the use of computed tomography and optical imaging that it is possible to produce copper parts with high density (approximately 98%) using laser powers below 500 W. The results also highlighted the difficulty in obtaining dense samples using various percentages of GNP, while the pure Cu samples were optimally processed.

Keywords: Copper; Graphene nanoplatelets; Laser power bed fusion

1. Introduction

The increasing use of laser powder bed fusion (L-PBF) technology in relevant sectors, including the medical, automotive, aerospace, and defense industries, is directing the market towards the demand for a wider range of materials able to meet the ever-increasing demands demanding of some sectors. In particular, copper and its alloys have always attracted the interest of the sectors of electronic devices, thermal management systems, and aerospace engine structures due to the excellent electrical and thermal conductivity of copper. The rapid development of modern electronics today often requires the copper component to have complex structures and precisely these new needs are directing the gaze of this sector towards the use of additive manufacturing (AM) technologies, in particular the L-PBF process. However, copper, due to its high reflectivity and thermal conductivity, is generally not a preferred raw material for L-PBF. Many researchers have pointed out that the main defects, such as porosity, cracks, low density, etc., found when processing copper and its alloys are caused by insufficient energy input due to the extremely high reflectivity of a 1.06 µm laser [1]. To overcome this problem, many studies have focused mainly on the acquisition of a greater supply of energy by replacing in L-PBF systems laser devices with higher power from the initial 200 W, to 400 W [2–4], then to 1 kW [1] and also 1.8 kW [5]. However, some studies [6,7] have shown that even with a laser power of 400 W, pure copper can be successfully fabricated by adjusting the process parameters (crack-free Cu parts with a density of 95%) and/or with an proper selection of the particle size distribution (PSD) of the powder [8]. However, although high-density levels are achieved, a pure copper part at full density could not be obtained and some lack-of-fusion defects were still detected. Another proposed alternative way to increase density is to increase the laser absorption of copper by using green or blue light laser (wavelength 515 nm and 450 nm respectively): infrared fiber laser (wavelength of 1064 - 1080 nm) absorb about 5% of the laser energy, while lasers in the visible spectrum absorb around 40-45% to the energy at room temperature independent of surface conditions. However, the

10.1016/j.procir.2023.06.111

mechanical and electrical properties of such parts produced with these lasers have not yet been reported. Another alternative solution is to modify the starting powder instead of the laser. Zhou et al. [9] found that the optical absorption of the powder can be significantly improved through a layered structure on the surface of the powder. Jadhav et al. [10] proposed an alternative approach to produce fully dense copper parts in L-PBF using an intentionally oxidized copper powder on the surface to improve the optical absorption at the fiber laser wavelength. The results showed a significantly higher optical absorption of 58% compared to 32% for virgin powder before oxidation. Dense parts exceeding 97.5 % using a laser power of 500 W were obtained. Moreover, the authors demonstrated that oxygen has a limited negative influence on the electrical conductivity of copper. Hu et al. [11] studied the fabrication of graphene-copper (Gr-Cu) nanocomposite using a custom L-PBF machine. The copper powders (d_{50} < 10 µm), graphene nanoplatelets (GNP; average x × y dimensions < 2 µm), and polyvinyl alcohol (PVA) were used to make two solutions. These were magnetically stirred at 120 °C for at least 12 h. The study revealed that the process was able to fabricate Gr-Cu nanocomposite and the addition of graphene improved the mechanical properties of the composites significantly. Carbon materials, generally used as reinforcement for composites in the form of particles, fibers, or whiskers, have, in fact, not only an exceptional thermal and electrical conductivity, but also a high Young's modulus and high tensile strength [12,13].

In this study, a comparison was made between pure copper and copper with GNP with the same process parameters to investigate the effect of GNP to improve the processability of copper using L-PBF machine with fiber lasers lower than 500 W. The laser manufacturing process involves a quick transition between the powder melting and the cooling phase which means that the melting and solidification time of the mixture is very short. Considering that the melting point of graphene (over 3000 °C [14]) is much higher than that of copper (1083.4 °C), remaining in the melting range of copper, GNP is not melted and copper does not react with it but this should increase its optical absorption so that the copper can be processed even with low laser powers.

2. Materials and methods

The samples were fabricated using gas atomized pure Cu powder. The morphological powder particles are shown in Fig. 1. The particle size of powder ranged from 15 to 53 µm.

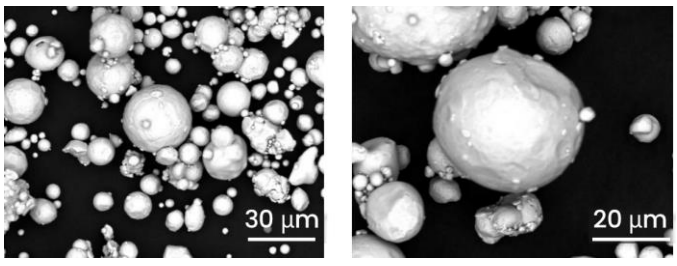

Fig. 1. Morphologies of copper powder.

GNP used is Alfa Aesar by Thermo Fisher Scientific with a purity higher than 99%. The average particle size is 7-11 µm.

In order to establish the correct amount of carbon to be added to pure copper without negatively affect its processability, six Cu-xGNP mixtures (x = 0.2, 0.4, 0.5, 1, 2, wt% GNP) were prepared, by mixing in a low energy jar mill for 24 – 72 hours.

First, a window of process parameters was identified for pure copper and subsequently, the same parameters were used to produce the samples of Cu-xGNP. For finding the optimal process parameters, various laser power (P), scan speed (v), hatching distance (h_d), and layer thickness (t) were applied in this work (Table 1). Energy densities (E_d) were calculated using Eq. (1) [15]:

$$E_d = \frac{P}{v \cdot h_d \cdot t} \qquad [\frac{J}{mm^3}] \tag{1}$$

The 10 mm side cubic specimens were produced on a stainless steel build platform. Two L-PBF systems, Concept Laser MLabR and Print Sharp 250, named in this study M1 and M2, were used. The M1 machine is equipped with a 100 W fiber laser and a focus beam diameter of approximately 50 µm. M2 machine works with a 500 W laser system and a spot size of 70-100 µm. The laser melting process is carried out in an argon atmosphere at oxygen content below 0.1% at a substrate temperature of 80 °C.

The flowability evaluation, performed through the Hall Flowmeter, and the spreadability test were conducted on the Cu-xGNP. The selected space between the roller and the plate was chosen equal to 20 µm. The plate used for this test was a stainless steel platform employed in the L-PBF process. In this way, it was possible to simulate the flowability and spreadability of the powder mixture. The spread layers, then, were analyzed at the stereomicroscope Leica S9i in order to identify the best possible solution. All the mixtures were analyzed at Scanning Electron Microscopy (SEM), with the Phenom PRO SEM machine.

Table 1. Process parameters used with the two different L-PBF machines.

Process parameters	M1	M2
Laser powder, P [W]	95	170 - 400
Scan speed v [mm/s]	134 - 200	300 - 2000
Hatching distance h_d [mm]	0.03 – 0.06	0.03 – 0.05
Layer thickness t [µm]	20	30
Energy density E_d [J/mm^3]	709.0-1181.6	222.22 – 740.74

3. Results and discussion

3.1 Characterization of mixtures.

From the analysis of the Hausner ratio (HR) on the pure Cu and mixtures, pure Cu shows an excellent flowability (1.0 < H < 1.1), while with the addition of even a small amount of GNP, the flow rate worsens drastically (HR >1.19 fair flowability). As for the spreadability test, pure Cu, thanks to the sphericity of the particles, shows a perfect uniform distribution over the

platform. By adding a small quantity of GNP, the spreadability is negatively affected (Fig. 2).

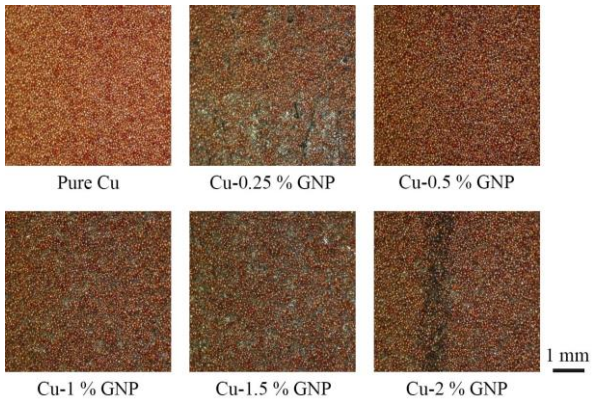

Fig. 2. Steromicroscope images of the spreaded layers.

An amount of GNP higher than 1.5 wt% tends to form agglomerates and, therefore, not to mix homogeneously with the copper. From this analysis, it was deduced that the best solution is to add 0.5% of GNP.

3.2 L-PBF process

The set of process parameters adopted for M1, both for pure Cu and for the mixtures, highlighted a series of problems. The production of the samples was stopped after 2.28 mm due to the formation of several balls on the surface. In the case of Cu-0.5% GNP (Fig. 3), the behavior was better than the other mixtures. Although combinations of parameters have been adopted to have a sufficient amount of energy to melt copper, laser power values lower than 100 W (Table 1) were unsuccessful in producing acceptable samples, highlighting the significance of this parameter.

In the case of the M2 system, balling occurred only in the case of the mixture, as opposed to pure Cu.

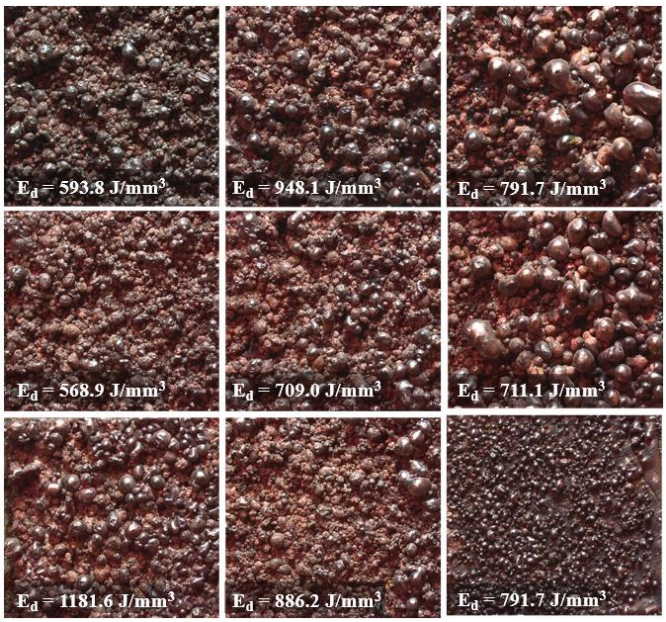

Fig. 3. Steromicroscope images of the Cu – 0.5 % GNP.

In the case of pure Cu, energy density values around 400 J/mm^3 have allowed the construction of samples with a density greater than 90% (Fig. 4a). With the same values, however, in the case of 0.4% and 0.5% of GNP, it was not possible to obtain dense components (Fig. 4b). In fact, there have been problems with balling, spatters, and keyholes. The phenomenon of balling causes the formation of discontinuous scanning traces and poor bonding properties between the hatching lines. Furthermore, it is a serious impediment to the uniform deposition of the powder on the previously sintered layer and tends to cause porosity and even delamination induced by poor bonding between the layers in combination with thermal stresses.

Although the same process parameters were used, the effect of GNP significantly worsened the fusion of the layer by creating many spatters. In current L-PBF machines, such spatters are mostly removed from the surface of the powder bed by a high-speed flow of shielding gas to prevent contamination of the powder bed. However, a significant portion of the metal ejections contaminate the surface of the powder bed or directly fall on the as-built metal, thus favoring metallurgical defects on the final parts as well as problematic during the coating of the subsequent layers. In the case of GNP, regardless of the percentage, there is a high spatter formation during laser radiation. Furthermore, the formation of these residual porosities indicates a certain instability typical of high energy densities and directly or indirectly related to the generation of spatters. The formation of keyholes typical in the L-PBF process for severe irradiation conditions (high E_d values) but without connection with process instability is also evident. However, the same issues occurred using lower energy values where the melt-pool spheroidizes under the action of surface tensions.

Instability regimes are also highlighted in the samples not only in the form of balling problems (Fig. 3) but also of humping. Humping, i.e. periodic formation of humps and valleys, has been attributed in the literature [16] to large fusion pool ratios (length/width) that generate Plateau-Rayleigh instability.

A high surface roughness during laser irradiation implies that the reflection of light on the surrounding environment is reduced. This results in an increase in the absorption rate. As a result, a high absorption rate results in a higher melt volume, thus leading to an effective welding process. However, this does not happen in the case of Cu-xGNP despite the melted layers having a higher roughness than that of pure copper. This can be a consequence of incorrect heat transfer between particles or of the presence of the high melting point graphene nanoplatelets, that limit the keyhole melting mechanism.

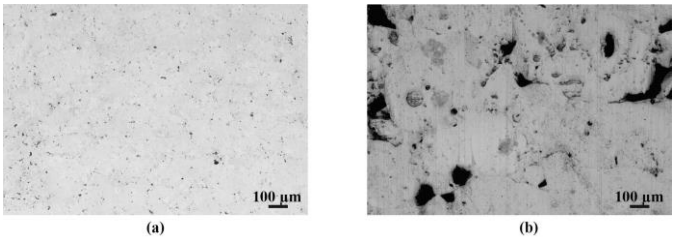

Fig. 4. (a) Pure Cu and (b) Cu-0.4% GNP samples.

The thermal conductivity reported in some studies on GNP/Cu composites is lower [17,18] or even degraded [19,20] with the addition of GNP, even when the second phase is uniformly dispersed in these composites. The main reason for the low efficiency of thermal conductivity improvement in graphene/metal composites is the lack of sufficient alignment of graphene in the metal matrix. Graphene has an in-plane thermal conductivity that is extremely superior to through-plane thermal conductivity [21]. Perfect alignment can maximize the contribution of thermal conductivity across the graphene plane by minimizing interfacial thermal resistance along the alignment direction, resulting in composites with exceptional in-plane thermal conductivity [22,23]. Therefore, well-ordered alignment and uniform dispersion are both essential to improve the thermal conductivity of the Cu-GNP composite. Moreover, thermal conductivity is an important thermophysical property in L-PBF because the ability of the powder to conduct heat will affect the consolidation process. During the process, the laser beam is irradiated to the powder surface and heat from the irradiated powder is conducted to other adjacent powder particles, in order to guarantee the total melting. Good consolidation occurs based on the appropriate amount of heat to melt powder particles so that they can fuse and form solid with surrounding powder particles. It seems that the presence of GNPs can limit the thermal conduction mechanism, thus reducing the melting of the copper particles and preventing the Cu-GNP composites to achieve full density.

4. Conclusion

In this study, the effects of adding different amounts of GNP to Cu powder were analyzed. Graphene is expected to help improve copper production via L-PBF. However, the results showed better processability of pure Cu compared to the Cu-xGNP mixture. In fact, the mixtures presented spreadability difficulties compared to pure Cu, so that the quantity and size of the graphene nanoplatelets must be carefully selected so as not to destroy the spreadability of the mixture. Furthermore, although different percentages of GNP were analyzed with different process parameters, the effects of balling, spatters, and keyholes were found in all samples. These problems may be due to incorrect heat transfer between the particles.

References

[1] Jadhav SD, Dadbakhsh S, Goossens L, Kruth JP, Van Humbeeck J, Vanmeensel K. Influence of selective laser melting process parameters on texture evolution in pure copper. J Mater Process Technol 2019. https://doi.org/10.1016/j.jmatprotec.2019.02.022.

[2] Zhang DQ, Liu ZH, Chua CK. Investigation on forming process of copper alloys via Selective Laser Melting. High Value Manuf. Adv. Res. Virtual Rapid Prototyp. - Proc. 6th Int. Conf. Adv. Res. Rapid Prototyping, VR@P 2013, 2014. https://doi.org/10.1201/b15961-53.

[3] Gustmann T, Schwab H, Kühn U, Pauly S. Selective laser remelting of an additively manufactured Cu-Al-Ni-Mn shape-memory alloy. Mater Des 2018. https://doi.org/10.1016/j.matdes.2018.05.010.

[4] Tian J, Zhu W, Wei Q, Wen S, Li S, Song B, et al. Process optimization, microstructures and mechanical properties of a Cu-based shape memory alloy fabricated by selective laser melting. J Alloys Compd 2019. https://doi.org/10.1016/j.jallcom.2019.01.153.

[5] Zhang S, Zhu H, Hu Z, Zeng X, Zhong F. Selective Laser Melting of Cu–10Zn alloy powder using high laser power. Powder Technol 2019. https://doi.org/10.1016/j.powtec.2018.10.002.

[6] Yan X, Chang C, Dong D, Gao S, Ma W, Liu M, et al. Microstructure and mechanical properties of pure copper manufactured by selective laser melting. Mater Sci Eng A 2020. https://doi.org/10.1016/j.msea.2020.139615.

[7] Constantin L, Wu Z, Li N, Fan L, Silvain JF, Lu YF. Laser 3D printing of complex copper structures. Addit Manuf 2020. https://doi.org/10.1016/j.addma.2020.101268.

[8] Sinico M, Cogo G, Benettoni M, Calliari I, Pepato A. Influence of powder particle size distribution on the printability of pure copper for selective laser melting. Solid Free. Fabr. 2019 Proc. 30th Annu. Int. Solid Free. Fabr. Symp. - An Addit. Manuf. Conf. SFF 2019, 2019.

[9] Zhou YH, Zhang ZH, Wang YP, Liu G, Zhou SY, Li YL, et al. Selective laser melting of typical metallic materials: An effective process prediction model developed by energy absorption and consumption analysis. Addit Manuf 2019. https://doi.org/10.1016/j.addma.2018.10.046.

[10] Jadhav SD, Vleugels J, Kruth JP, Van Humbeeck J, Vanmeensel K. Mechanical and electrical properties of selective laser-melted parts produced from surface-oxidized copper powder. Mater Des Process Commun 2020. https://doi.org/10.1002/mdp2.94.

[11] Hu Z, Chen F, Lin D, Nian Q, Parandoush P, Zhu X, et al. Laser additive manufacturing bulk graphene-copper nanocomposites. Nanotechnology 2017. https://doi.org/10.1088/1361-6528/aa8946.

[12] Lee C, Wei X, Kysar JW, Hone J. Measurement of the elastic properties and intrinsic strength of monolayer graphene. Science (80-) 2008. https://doi.org/10.1126/science.1157996.

[13] Lee C, Wei X, Li Q, Carpick R, Kysar JW, Hone J. Elastic and frictional properties of graphene. Phys Status Solidi Basic Res 2009. https://doi.org/10.1002/pssb.200982329.

[14] Zakharchenko K V., Fasolino A, Los JH, Katsnelson MI. Melting of graphene: From two to one dimension. J Phys Condens Matter 2011. https://doi.org/10.1088/0953-8984/23/20/202202.

[15] Prashanth KG, Scudino S, Maity T, Das J, Eckert J. Is the energy density a reliable parameter for materials synthesis by selective laser melting? Mater Res Lett 2017. https://doi.org/10.1080/21663831.2017.1299808.

[16] Gunenthiram V, Peyre P, Schneider M, Dal M, Coste F, Fabbro R. Analysis of laser–melt pool–powder bed interaction during the selective laser melting of a stainless steel. J Laser Appl 2017. https://doi.org/10.2351/1.4983259.

[17] Gao X, Yue H, Guo E, Zhang H, Lin X, Yao L, et al. Mechanical properties and thermal conductivity of graphene reinforced copper matrix composites. Powder Technol 2016. https://doi.org/10.1016/j.powtec.2016.06.045.

[18] Jagannadham K. Volume fraction of graphene platelets in copper-graphene composites. Metall Mater Trans A Phys Metall Mater Sci 2013. https://doi.org/10.1007/s11661-012-1387-y.

[19] Wejrzanowski T, Grybczuk M, Chmielewski M, Pietrzak K, Kurzydlowski KJ, Strojny-Nedza A. Thermal conductivity of metal-graphene composites. Mater Des 2016. https://doi.org/10.1016/j.matdes.2016.03.069.

[20] Boden A, Boerner B, Kusch P, Firkowska I, Reich S. Nanoplatelet size to control the alignment and thermal conductivity in copper-graphite composites. Nano Lett 2014.

https://doi.org/10.1021/nl501411g.

[21] Balandin AA. Thermal properties of graphene and nanostructured carbon materials. Nat Mater 2011. https://doi.org/10.1038/nmat3064.

[22] Renteria J, Legedza S, Salgado R, Balandin MP, Ramirez S, Saadah M, et al. Magnetically-functionalized self-aligning graphene fillers for high-efficiency thermal management applications. Mater Des 2015. https://doi.org/10.1016/j.matdes.2015.08.135.

[23] Chu K, Wang X hu, Wang F, Li Y biao, Huang D jian, Liu H, et al. Largely enhanced thermal conductivity of graphene/copper composites with highly aligned graphene network. Carbon N Y 2018. https://doi.org/10.1016/j.carbon.2017.10.099.